A new armored dinosaur with double cheek horns from the early Late Cretaceous of southeastern China

Lida Xing[1, 2], Kecheng Niu[3, 4], Jordan C. Mallon[5, 6], and Tetsuto Miyashita[5, 6, 7]*

[1]State Key Laboratory of Biogeology and Environmental Geology, China University of Geosciences, Beijing 100083, China
[2]School of the Earth Sciences and Resources, China University of Geosciences, Beijing 100083, China
[3]State Key Laboratory of Cellular Stress Biology, School of Life Sciences, Xiamen University, Xiamen 361105, China
[4]Yingliang Stone Natural History Museum, Nan'an, 362300, China
[5]Beaty Centre for Species Discovery & Palaeobiology Section, Canadian Museum of Nature, Ottawa, ON, Canada K1P 6P4
[6]Department of Earth Sciences, Carleton University, Ottawa, Ontario, Canada K1S 5B6; TMiyashita@nature.ca
[7]Department of Biology, University of Ottawa, Ottawa, Ontario, Canada K1N 9A7

Abstract: Ankylosaurines are the iconic armoured dinosaurs that characterize terrestrial vertebrate faunas in the Late Cretaceous of Asia and Laramidia (western North America). The earliest members of this clade are known from the early Late Cretaceous (Cenomanian–Santonian) times of Asia, but little consensus has emerged as to how they are related to the anatomically derived and chronologically younger forms. In southeastern China, the Cretaceous red sand beds crop out across basins from Zhejiang to Guandong provinces. However, the horizons corresponding to the early Late Cretaceous stages remain poorly sampled. Here, we report the first definitive vertebrate skeleton — let alone that of an armoured dinosaur — from the Coniacian/Turonian Ganzhou Formation, *Datai yingliangis* gen. et sp. nov. Despite the immature ontogenetic status of the type materials, *D. yingliangis* gen. et sp. nov. can be diagnosed with autapomorphic traits in the cranial caputegulae (such as double horns on the jugal/quadratojugal) and extensive gular osteoderms. Morphologically, it is intermediate between the chronologically older ankylosaurids from Asia (e.g., *Crichtonpelta* and *Jinyunpelta*) and derived post-Cenomanian ankylosaurines (e.g., *Pinacosaurus*). Phylogenetic analyses broadly corroborate this assessment. The new taxon either falls in the grade of Asian ankylosaurines proximal to the lineages of derived taxa or forms a sister lineage to *Pinacosaurus*. Based on these insights, *Datai* gen. nov. makes a significant addition to the early Late Cretaceous vertebrate fauna from southeastern China and highlights the future potential in this region for improved understanding of the origin and early evolution of ankylosaurines.

http://zoobank.org/urn:lsid:zoobank.org:act:16013E98-276B-44D6-A862-6A71F3F5D2CB

INTRODUCTION

Ankylosaurines (armoured dinosaurs with a tail club) reached the pinnacle of diversity in the latest Cretaceous Period (Campanian and Maastrichtian stages), but the record remains sparse in the preceding mid- Cretaceous times. Ankylosaurines known from the Albian to Santonian stages are dominated by Asian forms with loose chronological constraints: *Crichtonpelta* (Sunjiawan Formation, Cenomanian), *Jinyunpelta* (Liangtoutang Formation, Albian–Cenomanian), *Talarurus* (Baynshire Formation, Cenomanian), *Tsagantegia* (Baynshire Formation, Cenomanian–Santonian), and *Zhejiangosaurus* (Chaochuyan Formation, Cenomanian). There is no universal agreement that all these taxa represent ankylosaurines. *Zhejiangosaurus*, coeval with another poorly represented ankylosaur *Dongyangopelta*, was originally described as a nodosaurid (Lü et al. 2007b). *Talarurus* and *Zhejiangosaurus* fell outside the ankylosaurine clade in a recent analysis (Raven et al. 2023). Conventionally, *Shamosaurus* (Dzunbain Formation, Aptian–Albian) is used as an outgroup to the Ankylosaurinae (Vickaryous et al. 2004; Thompson et al. 2012; Arbour and Currie 2016). *Gobisaurus* (Ulansuhai Formation, Turonian) is often allied with *Shamosaurus* in a clade (Vickaryous et al.

2001, 2004; Arbour and Currie 2016; Yang et al. 2017; Arbour and Evans 2017; Rivera-Sylva et al. 2018; Kuzmin et al. 2020; Raven et al. 2023), as successive branches in a grade (Thompson et al. 2012; Han et al. 2014; Yang et al. 2017), or in a polytomy (Zheng et al. 2018). Other mid-Cretaceous ankylosaurs fall among non-ankylosaurine ankylosaurids in some analyses. These are *Cedarpelta* (Cedar Mountain Formation, Aptian–Albian) (Thompson et al. 2012; Han et al. 2014; Arbour and Currie 2016; Arbour and Evans 2017; Rivera-Sylva et al. 2018; Zheng et al. 2018; Kuzmin et al. 2020), *Dongyangopelta* (Chaochuyan Formation, Cenomanian) (Raven et al. 2023), *Kunbarrasaurus* (Toolebuc Formation, Albian) (Hill et al. 2003; Vickaryous et al. 2004; Thompson et al. 2012; Han et al. 2014; Arbour and Evans 2017; Raven et al. 2023), and *Zhongyuansaurus* (Haoling Formation, Aptian–Albian) (Thompson et al. 2012). The taxonomic validity of *Zhongyuansaurus* has been questioned (Arbour and Currie 2016), whereas two species of *Crichtonpelta* are considered synonymous (Arbour and Currie 2016).

Overall, these mid-Cretaceous ankylosaurs appear to be derived from various points of the transition toward the post-Santonian ankylosaurines. These post-Santonian ankylosaurines are generally distinguished from non-ankylosaurine ankylosaurids by large body size, transversely wide skull and body profiles, and a prominent tail club (Vickaryous et al. 2004). However, this transition remains poorly resolved because of phylogenetic instability near the base of the Ankylosaurinae coupled with insufficient record in the mid-Cretaceous stages.

As a significant addition to a small number of mid-Cretaceous ankylosaurids, here we report a new ankylosaurine from the Coniacian–Turonian (early Late Cretaceous) of southeastern China. The specimens were collected from the Zhoutian Formation (the Ganzhou Group) from which no vertebrate body fossils have previously been reported. Instead, the Zhoutian Formation has yielded a large number of dinosaur eggs (Zou et al. 2013; Yu et al. 2020; Yu and Fan 2022). The new ankylosaurine is represented by two well preserved immature skeletons, each showing a slightly different set of ontogenetic traits. We present an anatomical diagnosis of this new taxon with a focus on comparison to *Jinyunpelta*, *Pinacosaurus*, and other Asian ankylosaurines. Phylogenetic analyses find it nested within a grade of Asian ankylosaurids, but this topology is obtained after extensive pruning of an existing dataset.

Institutional Abbreviations: IGM, Geological Institute of Mongolia, Ulanbaatar, Mongolia; IVPP, Institute of Vertebrate Paleontology and Paleoanthropology, Beijing, China; YLSNHM, Yinliang Stone Natural History Museum, Shuitou, China; ZPAL, Institute of Paleobiology, Polish Academy of Science, Warsaw, Poland.

SYSTEMATIC PALAEONTOLOGY

Dinosauria Owen, 1842
Ornithischia Seeley, 1887
Thyreophora Nopcsa, 1915
Ankylosauria Osborn, 1923
Ankylosauridae Brown, 1906

Datai gen. nov.
Type and Only Known Species: *Datai yingliangis* sp. nov.
Etymology: '*Datai*,' a composite of the last character (syllable) each from tongda (to understand/to be sensible) and antai (stable) in Chinese Pinyin.
Diagnosis: as for type and only known species.

Datai yingliangis sp. nov.
Figures 3–5
Holotype: YLSNHM 01002: skull, anterior presacral series, ribs, distal caudal vertebrae, pectoral girdles, left forelimb, partial left ilium, distal right femur, trunk osteoderms (Figs. 3A–G, 4G–J, 5A, B).
Paratype: YLSNHM 01003: skull, anterior presacral series, pectoral girdles, left elbow (distal humerus, proximal radius, proximal ulna), trunk osteoderms (Figs. 3H–K, 4A–F, 5C–E).
Etymology: '*yingliangis*', in recognition of the Yingliang Group. The Yingliang Stone Natural History Museum is operated as a public museum by the philanthropic program of the founder (Liang Liu) of the Yingliang Group, and the type specimens are curated in this museum in Shuitou, Fujiang, China.
Type locality and horizon: Zhoutian Formation, Ganzhou Group (Turonian–early Coniacian; Upper Cretaceous; 96–90 Ma).
YLSNHM 01002 and YLSNHM 01003 were found in Mazhou, Huichang County, Jiangxi Province, People's Republic of China, approximately 90 km east-southeast of Ganzhou City (Fig. 1). The locality is at 25°30'25.86"N, 115°46'33.99"E. The fossils were exposed in 2016 during road construction along the Gongshui River and reported by workers as preserved in a boulder from the spoil pile of explosive excavation. The original horizon is subterranean as it is now a buried construction site. The Yingliang Stone Natural History Museum obtained the specimens in 2018, and the first author (L.X.) revisited the locality to confirm the provenance and document the geological horizon.

The horizon belongs to the third unit within the Ganzhou Group, which is dominated by siltstone and mudstone and grading into conglomerate in the local facies (Jiangxi Geological Survey and Mineral Survey Brigade 1991). The Cretaceous red beds of Jiangxi Province used to be considered contiguous with the Nanxiong Group (Bureau of Geology
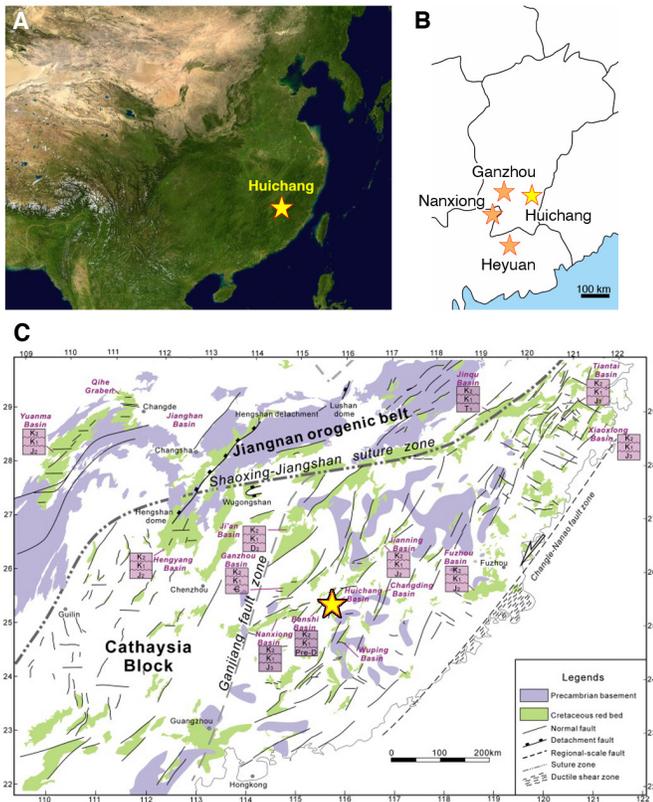
Figure 1. Geological and geographical contexts for the type locality of *Datai yingliangis*. The type locality is indicated by a yellow star. A, Location of the Huichang Basin (the original map provided by NASA Worldwind). B, Jiangxi and its neighboring provinces with major localities of the Nanxiong Group/Formation (map modified after https://d-maps.com/). C, Surface geological map of Jiagxi, Guangdong, and Fujian provinces modified from Figure 4 of Li et al. (2014) (green = Cretaceous red beds; purple: Precambrian basement) with solid lines representing fault lines. The type locality sits within the Huichang Basin.

and Mineral Resources of Jiangxi Province 1984), which is broadly exposed in the Nanxiong Basin of the neighbouring Guangdong Province. This traditional scheme has been since revised. From the bottom to the top, the red beds are now classified as the Lower Cretaceous Wuyi and Huobashan groups and the Upper Cretaceous Ganzhou and Guifeng groups (Jiangxi Bureau of Geology and Mineral Resources 1987; Ling 1996). The Ganzhou Group is further subdivided into the Maodian and Zhoutian formations, whereas the Guifeng Group consists of the Hekou, Tangbian, and Lianhe formations (Jiangxi Bureau of Geology and Mineral Resources 1997; Wu et al. 2020). Zircon dating placed the lower Maodian Formation to after the early Albian stage (110 Ma), and the Zhoutian Formation to the Turonian to early Coniacian stages (96–90 Ma) (Li et al. 2018; Wu et al. 2020). It is possible that the Zhoutian Formation represents roughly contemporaneous but allogenic deposition with the overlying Hekou Formation (Li et al. 2018). The Zhoutian Formation is generally interpreted as a shallow lacustrine assemblage, whereas the Hekou

Formation was likely deposited in a mesoalluvian fan (Yu and Fan 2022). Skeletal fossils from the Mazhou site are preserved in reddish-brown clastic sandstones in the upper part of the Zhoutian Formation, and the clastic grain size is significantly finer than that of the Hekou Formation.

Diagnosis: An ankylosaurine with dual jugal/quadratojugal horns. This taxon is also distinguished from all other ankylosaurines with a unique combination of the following characters: protruded premaxilla such that prenarial portion is longer than infranarial portion (also present in *Zhongyuansaurus luoyangensis*), distinct 'postfrontal' caputegulum (also in *Pinacosaurus mephistocephalus* and *Talarurus plicatospineus*), well-developed supraorbitals forming no lacrimal incisure or postorbital peak (potentially controlled ontogenetically), parasagittaly projecting squamosal horn (also in *Scolosaurus cutleri/Oohkotokia horneri*), nuchal horn (also in A*nkylosaurus magniventris, Euoplocephalus tutus, Nodocephaosaurus kirtlandensis, Zuul crurivastator*), and polygonal, monotypic gular osteodrms covering the intermandibular region and the entire throat (polymorphic gular osteoderms occur in *Jinyunpelta sinensis*).

DESCRIPTION

The two specimens (YLSNHM 01002, YLSNHM 01003) were found in association (Fig. 2) and represent slightly different stages of skeletal ontogeny (the underlying YLSNHM 01002 is better ossified). In each specimen, dermal elements in the skull maintain open sutures on all sides. In YLSNHM 01002, the sutures were closing at the time of death but remain traceable between the jugal and the postorbital, between the squamosal horn and the underlying squamosal (on the right side), among the supraorbitals (on the right side), and among the caputegulae along the posterior margin of the skull. Neurocentral sutures are open in both specimens. The coracoid and scapula are preserved in association but disarticulated. Caputegulae had begun to ossify in both specimens at the time of death. These are better developed in YLSNHM 01002. Overall, the degrees of ossification in these specimens are similar to subadult specimens of *Pinacosaurus grangeri* (IGM 100/1014; ZPAL MgD-II/1) (Maryańska 1971, 1977; Hill et al. 2003) and are more advanced in caputagular development than juvenile specimens of the same species (IVPP P16283, IVPP P16853; PIN 3144/49/1-4) described by Burns and colleagues (Burns et al. 2011, 2015). Measurements are given in Appendix 1.

Skull: In overall appearance, the skulls of *Datai yingliangis* (Fig. 3) resemble those of immature individuals of *Pinacosaurus grangeri* (Maryańska 1971; Hill et al. 2003; Burns et al. 2011): the occiput is wide and the preorbital length is semi-equal to the rest of skull length. However, the two species differ in three important features in the snout. In *D. yingliangis*, the snout becomes progressively narrower anteriorly to terminate in a round premaxillary beak. In lateral

Figure 2. The type specimens of *Datai yingliangis* gen. et ap. nov. (individual lying on top: YLSNHM 01003; individual on bottom: YLSNHM 01002, holotype) prepared and reconstructed in situ. The head, cervical, and thoracic regions of the specimens were discovered and extracted from a single block.

view, the premaxilla protrudes anteriorly such that the prenarial portion is longer anteroposteriorly than the rest of the bone. *D. yingliangis* also lacks the lacrimal incisure common among ankylosaurines, where the skull outline is discontinuous from the orbit to the snout in dorsal view. These differences are still apparent when comparing *D. yingliangis* with the earliest ontogenetic stages known in *P. grangeri* (Burns et al. 2011). The orbit occupies well more than half the skull length behind the lacrimal in juveniles and subadults of *P. grangeri*, but this is not the case in *D. yingliangis* (YLSNHM 01002) in which the diameter of the orbit is approximately 20% of the skull length and subequal to the horizontal dimension of the temporal bar.

Despite being collected from much younger sediments and nearly 600 km southwest in a separate basin, the skulls of *Datai yingliangis* (Fig. 3) also appears similar to that of *Jinyunpelta sinensis*, an ankylosaurine from the Albian-Cenomanian of the neighboring Zhejiang Province (Zheng et al. 2018). The superficial resemblance is mainly driven by common preservation styles. The skulls of *D. yingliangis* and *J. sinensis* are both crushed dorsoventrally, embedded in reddish sandstone, and preserved with extensive tiling of gular osteoderms. However, a close look reveals many differences. The snout of *D. yingliangis* differs from that of *J. sinensis* in the same traits used to distinguish the former

from *Pinacosaurus grangeri* (outlined in the previous paragraph). Additionally, there is no evidence in *D. yingliangis* for the maxillary and antorbital fossae along the anterodorsal and posterodorsal margins of the maxilla, respectively, or for two "oval cavities" on the nasal, which are all considered diagnostic to *J. sinensis* (Zheng et al. 2018:3). In *D. yingliangis* and *P. grangeri*, the lacrimal contacts the nasal to exclude the prefrontal from the dorsal margin of the maxilla (Maryańska 1971, 1977; Burns et al. 2011), whereas in *J. sinensis* the prefrontal has a broad contact with the maxilla (Zheng et al. 2018).

The skull of the holotype of *Datai yingliangis* (YLSNHM 01002: Fig. 3A–G) is approximately two thirds the length of that of *Jinyunpelta sinensis*, but more caputegulae occur in the former. In YLSNHM 01002, the lacrimal, supraorbital, postfrontal, and nuchal caputegulae are clearly differentiated. The lacrimal caputegulum occupies only about half the area of the lacrimal but would have grown larger as the animal aged, given the overall incomplete state of ossification in this specimen. Three unfused elements form the supraorbital series. The posterior supraorbital has a sharp edge along the outline of the skull roof in both *D. yingliangis* and *J. sinensis*, but only in the latter it develops a distinct peak (Zheng et al. 2018). A prominent dermal ossification sits on the squamosal and parietal in
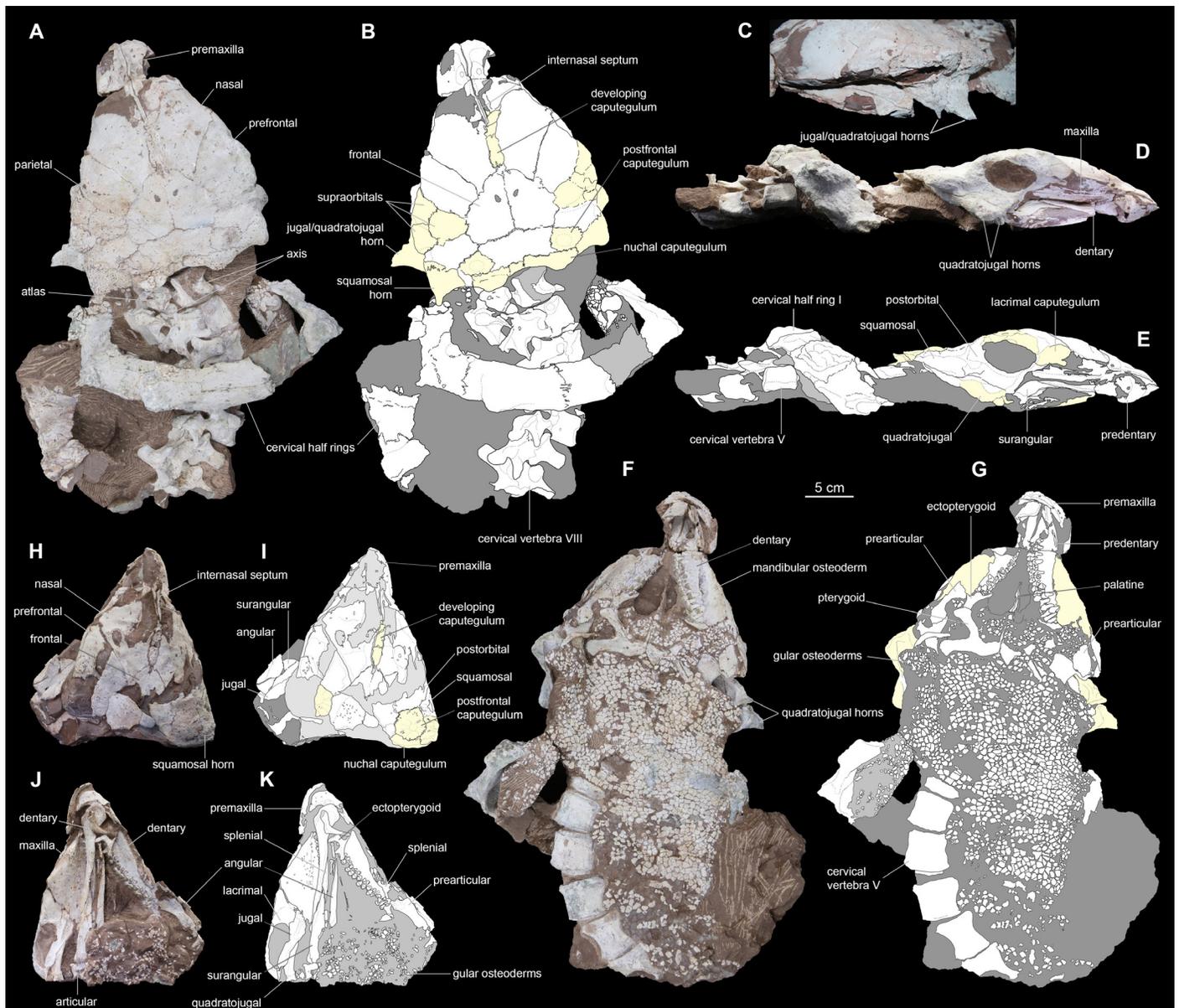
Figure 3. The skulls of the type specimens of *Datai yingliangis*. A–F: YLSNHM 01002. A, B, dorsal view in photograph (A) and interpretive drawing (B). C, left lateral view in photograph, showing the double jugal/quadratojugal horns. D, E, right lateral view in photograph (D) and interpretive drawing (E). F, G, ventral view in photograph (F) and interpretive drawing (G). H–K, YLSNHM 01003. H, I, dorsal view in photograph (H) and interpretive drawing (I). J, K), ventral view in photograph (J) and interpretive drawing (K). Caputegula developing in association of the skull are shaded with pale yellow in the interpretive drawings. All panels to scale. Roman numerals represent numbers on meristic structures such as vertebrae.

both YLSNHM 01002 and YLSNHM 01003 (Fig. 3A, B, I, J). This element corresponds to what has been labeled "postfrontal" in *Pinacosaurus mephistocephalus* (Godefroit et al. 1999:22) and "anterolateral nuchal caputegulum" in *Talarurus plicatospineus* (Park et al. 2020:5). In *D. yingliangis* and *P. mephistocephalus*, the caputegulum is clearly not a part of the nuchal series, so this element is hereby identified as the postfrontal caputegulum. As a distinct element, the caputegulum occurs in just a few ankylosaurines and may form open sutures with — and thereby distinguished from — the squamosal, parietal, and sur-

rounding caputegula. The latter condition is present in *D. yingliangis* and *P. mephistocephalus* only. There is a single nuchal caputegulum on each side as in most other Asian ankylosaurines (but unlike *T. plicatospineus* and Laramidian ankylosaurines). It develops a small horn on the nuchal edge (Fig. 3A, B) as in *T. plicatospineus, Tsagantegia longicranialis*, and many Laramidian ankylosaurines, but Asian ankylosaurines generally lack this feature.

Datai yingliangis is unique for having two jugal/quadratojugal horns (Fig. 3C–G). The main horn develops in the posteroventral corner of the skull, projecting posterolat-

117

erally. The smaller accessory horn sits just anterior to this and obscures the jaw joint from lateral view. The temporal region is inclined posterodorsally in *D. yingliangis*. As in *Saichania chulsanensis* (but unlike most other ankylosaurines) the orientation parallels the similarly inclined shaft of the quadrate (Maryańska 1977). The gular osteoderms in *D. yingliangis* are small, polygonal, and monotypic, whereas those in *J. sinensis* (Zheng et al. 2018) vary in size and shape and distribute heterogeneously, with the larger scales more frequent between the left and right jaw joints. These morphological differences discussed here with respect to *J. sinensis* and *P. grangeri* can be used in various combinations

to also distinguish *D. yingliangis* from other ankylosaurines.

Postcranial Skeleton: A full cervical series and the first five dorsal vertebrae are preserved in articulation in YLSNHM 01003 (Fig. 4A–F). In addition, four dorsal vertebrae are preserved in articulation on each of two blocks of YLSNHM 01002 (Fig. 4G–I). The neurocentral sutures remain open on these vertebrae (Fig. 4I), again indicating the immature ontogenetic status for these specimens (Coombs 1986; Burns et al. 2015). The middle (III–V) cervical vertebrae of YLSNHM 01003 are penetrated by two sinuous burrow casts from the right side (Fig. 4C–F). Both casts invaded the neural canal through the open neuro-
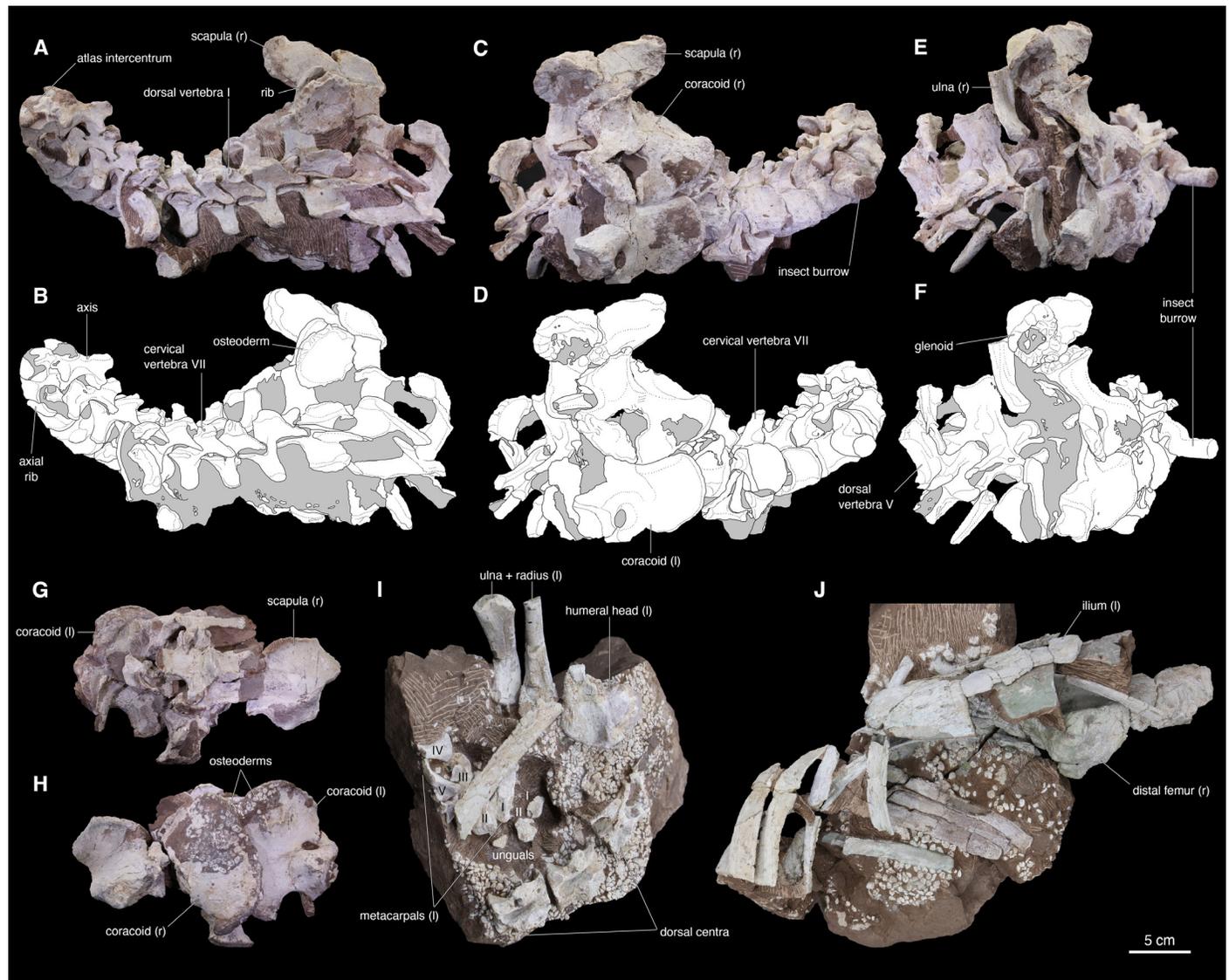
Figure 4. The postcranial blocks of the type specimens of *Datai yingliangis*. A–F: YLSNHM 01003, cervical and thoracic series with pectoral girdles. A, B, Left lateral view in photograph (A) and interpretive drawing (B). C, D, Right lateral view in photograph (C) and interpretive drawing (D). E, F, Posterior view in photograph (E) and interpretive drawing (F). Burrow casts are visible from the right side. G–J: YLSNHM 01002 in multiple blocks. G, H, Pectoral girdles with thoracic vertebrae in dorsal (G) and ventral (H) vies. (I) Left forelimb (elbow region missing) and dorsal centra revealing the open neurocentral sutures. The elbow region is missing. J, Posterior ribcage and fragments of the pelvic girdle (left ilium) and hindlimb (right distal femur). All blocks are preserved with osteoderms. Roman numerals represent numbers on meristic structures such as digits and vertebrae. (l) = left side; (r) = right side. All to scale.

central sutures. Each with the diameter of approximately 2 cm, the burrows appear to be a trace made by beetles, possibly foraging on soft tissues, laying eggs, or digging pupation chambers (Britt et al. 2008; Kirkland and Bader 2010; Xing et al. 2013). Unlike feeding traces attributed to termites in other dinosaur skeletons (Britt et al. 2008; Kirkland and Bader 2010; Backwell et al. 2012; Xing et al. 2013; Li et al. 2016; Serrano-Brañas et al. 2018), there is no other apparent evidence for bone-foraging activities such as pitting, boring, or trenching across the bone surfaces around the burrow casts of YLSNHM 01003. A block of four distal caudal vertebrae is associated with YLSNHM 01002 (Fig. 5A, B). These vertebrae are interlocked by long postzygapophyses that extend more than half the length of the next segment, wrapped on lateral sides by ossified tendons, and supported ventrally by longitudinally elongate haemal arches. These "handle" vertebrae reinforced by ossified tendons are generally associated with the presence of a tail club (Coombs 1978). Although these vertebrae evolved before the tail club within ankylosaurs (Arbour and Currie 2015), comparison with *Jinyunpelta sinensis* (Zheng et al. 2018) implies that the terminal structure was likely present in *Datai yingliangis*.

The shoulder girdles are incompletely preserved in pair in
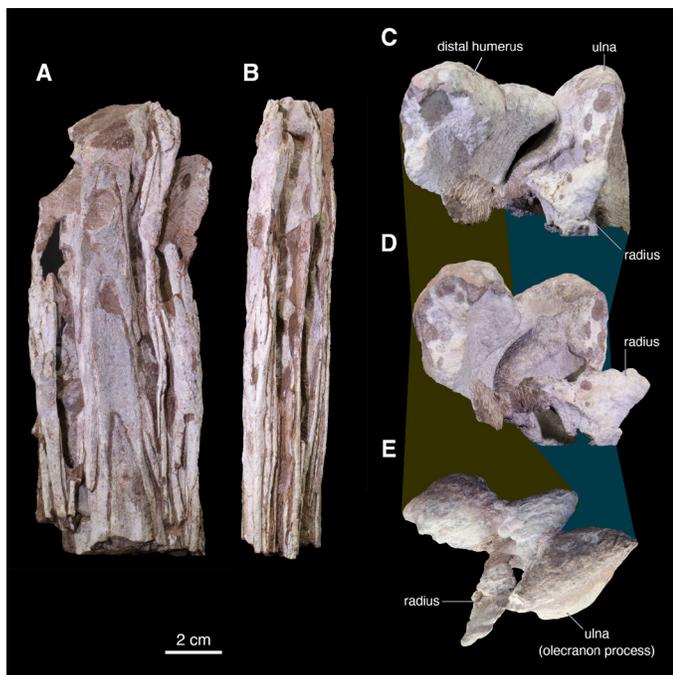
Figure 5. Additional postcranial elements of the type specimens of Datai yingliangis. A, B, YLSNHM 01002, distal caudal series in dorsal (A) and right lateral (B) views. C–E, YLSNHM 01002, right lateral elbow region with distal humerus, proximal ulna, and proximal radius preserved in flexed articulation in medial (A), anterior (B), and proximal/distal (E) views.

both YLSNHM 01002 (Fig. 4G, H) and YLSNHM 01003 (Fig. 4A–F). The coracoid has a round anterior edge and a prominent sternal process, which differs from the flat profile typical of Laramidian ankylosaurines but is similar to the condition seen generally among Asian ankylosaurines. The anterodorsal process of the coracoid is only a thickening at the origin of the biceps as in juveniles of *Pinacosaurus grangeri* (Burns et al. 2015), whereas in *Crichtonpelta benxiensis* (Lü et al. 2007a) and *Shamosaurus scutatus* (Tumanova 1987) the process forms an apex off the main body of the bone. Unlike the gently concave profile in *P. grangeri*, the sternal process and the lip of the glenoid are close to each other and only separated by the sharply crescent posterior margin. The preserved portion of the scapula shows that the acromion is less pronounced than in juveniles of *P. grangeri* and similar to the condition in *C. benxiensis* and *Jinyunpelta sinensis*. Unlike most ankylosaurines but similar to nodosaurids (Coombs 1995), the scapular blade is weakly constricted in width after the acromion. The forelimbs are partially preserved. In YLSNHM 01002, the humeral head and the distal two thirds each of the radius and ulna are preserved on the same block with the right manus (thus missing the elbow and much of the upper arm) (Fig. 4I). The elbow region is preserved in YLSNHM 01003 (Fig. 5C–E). The olecranon process of the ulna is prominent but slender, with its maximum height subequal to the distal humeral width. An anterior portion of the left iliac blade and the distal third of the right femur are preserved in YLSNHM 01002 (Fig. 4J), but there is little information useful for systematic comparison.

Datai yingliangis has two cervical half rings as preserved in YLSNHM 01002 (Fig. 3A, B, D, E). Like other ankylosaurines, each half ring consists of six osteoderms, three on each side. The sutures between the osteoderms are not fully closed. Although the horns on the skull are distinct in this specimen, each osteoderm does not form an apparent apex but is instead thickened into a boss. In addition to the gular rosettes, YLSNHM 01002 is preserved with numerous ossified scales ranging in size from 2 mm to 1 cm in diameter (Figs. 3F, G, J, K; 4H–J). The scale morphology is homogeneous over the coracoids and around the hip (monotypic polygons with a diameter around 5 mm) and more heterogenous (variable shapes and sizes without apparent tiling patterns) on the block with the dorsal vertebrae and the right forelimb.

PHYLOGENETIC ANALYSES

The ankylosaurian phylogeny remains unstable. Numerical cladistic analyses over the last three decades have generated various hypotheses of interrelationships (Kirkland 1998; Carpenter 2001; Hill et al. 2003; Vickaryous et al. 2004; Osi

2005; Thompson et al. 2012; Han et al. 2014; Wiersma and Irmis 2018; Norman 2021; Soto-Acuña et al. 2021; Yao et al. 2022; Riguetti et al. 2022b, 2022a; Raven et al. 2023), but in recent times these datasets converged onto the three independent lines of research rooted in Arbour and Currie (2016), Wiersma and Irmis (2018) and Raven et al. (2023). The common feature between them is that the ankylosaurian relationships are so unstable that, in these maximum parsimony analyses, consensus is typically obtained by majority rule. Strict consensus tends to collapse many internal nodes unless the dataset is extensively pruned (Arbour and Currie 2013, 2016; Yang et al. 2017; Wiersma and Irmis 2018; Zheng et al. 2018; Raven et al. 2023). Even the internal ankylosaur nodes resolved under strict consensus are one extra step away from collapsing (Bremer support/decay index = 1). Nevertheless, there is an emerging consensus that: a) ankylosaurids (all ankylosaurs closer to *Ankylosaurus magniventris* than to *Panoplosaurus mirus*; Sereno 1998) contain a grade of Early to Late Cretaceous taxa, most of which lacked a tail club; b) within ankylosaurines (all ankylosaurids closer to *Ankylosaurus magniventris* than to *Shamosaurus scutatus*; Sereno 1998), the early-branching lineages occur in Asia; and c) derived ankylosaurines from the Campanian to Maastrichtian of Laramidia may form a clade (= Ankylosaurini, sensu Arbour and Currie 2016), mostly endemic to that continent.

The Dataset Based on Arbour & Currie (2016):

Our analysis produced results consistent with these general insights above. We scored *Datai yingliangis* on the dataset of Zheng et al. (2018), which is a version of the dataset from Arbour and Evans (2017) with the addition of *Jinyunpelta sinensis*. For the purpose of this paper, a maximum parsimony analysis of the dataset of Arbour and Evans (2017), modified from Zheng et al. (2018), found *Datai yingliangis* in a grade of Asian lineages within the Ankylosaurinae. Under heuristic search on PAUP our initial analysis of the total dataset resulted in a collapse of most internal nodes under strict consensus. Therefore, we deleted 14 taxa that are less than 20% complete ("Argentinean ankylosaur", *Dongyuangopelta yangyanensis*, *Nodosaurus textilis*, "Paw Paw scuteling", *Hoplitosaurus marshi*, *Sauroplites scutiger*, *Stegopelta landerensis*, *Struthiosaurus languedocensis*, *Struthiosaurus transylvanicus*, *Taohelong jinchengensis*, *Texasetes pleurohalio*, *Ahshislepelta minor*, *Aletopelta coombsi*, *Zhejiangosaurus luoyangensis*), modified the coding for a single character in two species of *Pinacosaurus* (Character 53: number of nuchal caputegulae, from "?" to "1"), and re-ran the analysis. Even though highly incomplete taxa can improve both precision and accuracy of the tree hypotheses (Wiens 2003a, 2003b, 2005; Wiens and Tiu 2012), for this paper we prioritize

forming a robust phylogenetic hypothesis for *Datai*. Safe taxon removal has been applied to the previous version of this dataset but did not lead to substantial improvement of resolution (Arbour and Currie 2016).

This analysis returned 392 MPTs at tree length = 554 (consistency index = 0.406; retention index = 0.659). Strict consensus (Fig. 6A) presents well-resolved Ankylosauridae, where *Datai* is nested within the Ankylosaurinae and outside the least inclusive clade containing *Ankylosaurus* and *Pinacosaurus*. Behind *Datai*, successive outgroup lineages are the clade (*Crichtonpelta* + *Jinyunpelta*), shamosaurines (*Gobisaurus* + *Shamosaurus*), and the Early Cretaceous non-nodosaurid forms (*Cedarpelta*, *Chuanqilong*, *Liaoningosaurus*) in a polytomy. The more derived forms are split into the exclusively Gobi clade (*Tsagantegia* + (*Saichania* + (*Tarchia* + *Zaraapelta*))) and the largely Laramidian clade. In the latter clade, *Dyoplosaurus* and the (*Nodocephalosaurus* + *Talarurus*) clade form successive outgroups to the remaining ankylosaurines. The panoplosaurin clade is not recovered among nodosaurids. Another seemingly bizarre outcome of this analysis is that *Gargoyleosaurus, Hylaeosaurus, Kunbarrasaurus*, and *Mymoorapelta* form a grade outside the Euankylosauria (Ankylosauridae + Nodosauridae). These taxa are known to be unstable and have shifted positions radically across the previous analyses. Particularly, *Kunbarrasaurus* has been resolved as the outgroup to all other ankylosaurs (Kirkland 1998; Carpenter 2001; Arbour and Currie 2016; Wiersma and Irmis 2018), a parankylosaur (Soto-Acuña et al. 2021; Riguetti et al. 2022b), an ankylosaurid (Vickaryous et al. 2004; Thompson et al. 2012; Han et al. 2014), or an ankylosaurine (Hill et al. 2003). The other three have fallen into the 'polacanthine' clade, inside nodosaurids, within ankylosaurids, or as non-euankylosaurian ankylosaurs in various combinations (Kirkland 1998; Carpenter 2001; Hill et al. 2003; Vickaryous et al. 2004; Thompson et al. 2012; Arbour and Currie 2016; Wiersma and Irmis 2018). This analysis differs from the previous ones in having all four resolved in a basal ankylosaurian grade.

We repeated maximum parsimony analyses by restoring one taxon for each of the 14 removed taxa. We also ran another set of secondary parsimony analyses by restoring a pair of deleted taxa, for each pairwise combination of the deleted taxa that are 10–20% complete. These deleted taxa include those known to be highly incomplete and unstable but potentially important as a calibration point for the ankylosaurid, ankylosaurine, or ankylosaurin node, such as *Aletopelta*, *Ahshislepelta*, and *Zhejiangosaurus*. None of these secondary analyses improved the resolution of the strict consensus after 14 taxon deletions (Fig. 6), but these modifications resulted in various combinations of different
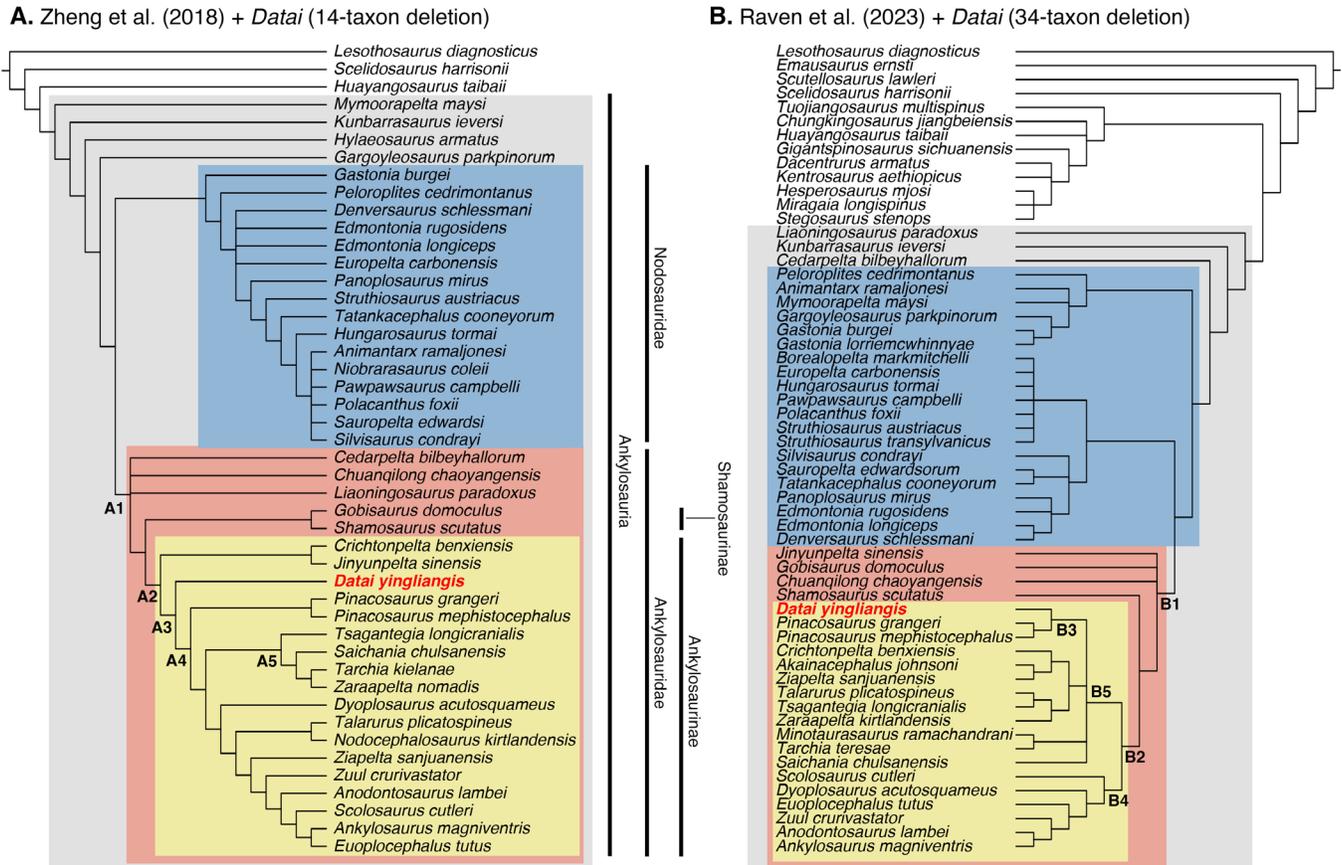
Figure 6. Phylogenetic analyses to resolve the position of *Datai yingliangis*. A, strict consensus of the 392 most parsimonious trees resulting from a heuristic search based on the reduced dataset after the deletion of 14 taxa (see text for analytical details and Supplementary Information for the source data). *Datai yingliangis* is nested within the Ankylosaurinae and in a grade of Asian forms. Tree length = 554; consistency index = 0.406; retention index = 0.659. B, strict consensus of the 840 most parsimonious trees resulting from a heuristic search based on the reduced dataset after the deletion of 34 taxa (see text for analytical details and Supplementary Information for the source data). *Datai yingliangis* is resolved as a sister lineage to *Pinacosaurus* spp. Tree length = 1335; consistency index = 0.303; retention index = 0.516.

topological relationships for *Gargoyleosaurus*, *Hylaeosaurus*, *Kunbarrasaurus*, and *Mymoorapelta*.

The Dataset Based on Raven et al. (2023):

To gain consensus on the phylogenetic position of *Datai yingliangis*, we also score this new taxon on the dataset of Raven et al. (2023), which is the most recent and comprehensive matrix currently available. First, we ran heuristic search on the whole dataset using PAUP* (Swofford 2017). This collapsed most internal nodes, including the thyreophoran, eurypodan, stegosaurian, ankylosaurian, euankylosaurian, ankylosaurid, and anlylosaurine nodes. This is expected given multiple parallel analyses done on the original dataset to obtain broad consensus (Raven et al. 2023). As a useful concept, Raven et al. (2023) offer a "signal tree" in which taxa that are less than 25% complete in character scores were deleted from the maximum parsimony analysis. We relaxed the 25% completeness threshold to 20%

(which deleted 34 taxa) and re-ran the analysis with *Datai yingliangis* under the same setting. The analysis included 58 taxa and 340 characters and found 840 most parsimonious trees at length = 1335, with consistency index = 0.303 and retention index = 0.516. Strict consensus of these trees (Fig. 6B) shows that *Datai* is resolved in a clade with the two species of *Pinacosaurus*, nested within the Asian clade of ankylosaurines (with the exception of *Akainacephalus* and *Ziapelta*). *Crichtonpelta* is also nested within this clade. In Arbour and Currie (2016) and subsequent analyses (Arbour & Evans, 2017; Zheng et al., 2018), *Talarurus* tends to be allied with *Nodocephalosaurus*. Here, however, it is nested in an entirely Mongolian clade with *Tsagantegia* and *Zaraapelta*. Outside the Ankylosaurinae, shamosaurines (*Gobisaurus* + *Shamosaurus*) collapsed into a grade, and *Jinyunpelta* fell in a polytomy with *Chuanqilong* and *Gobisaurus*. Outside the Ankylosauridae, the result of this analysis is consistent with the findings of Raven et al.

(2023) for nodosaurids to represent a grade. The typically unstable taxa such as *Gargoyleosaurus* and *Mymoorapelta* are nested among the taxa conventionally considered as nodosaurids (*Animantarx, Gastonia, Peloroplites*), whereas *Cedarpelta, Kunbarrasaurus*, and *Liaoningosaurus* occupy positions corresponding in other analyses to non-euankylosaurian ankylosaurs.

DISCUSSION

Phylogeny of Ankylosaurs and Systematic Implications for *Datai*:

The two lines of maximum parsimony analyses produced dissimilar consensus trees (Fig. 6). The differences largely concern: a) 'nodosaurids' as a clade or a grade; and b) the individual taxa known to be unstable in previous analyses among 'nodosaurids', non-euankylosaur ankylosaurs, and non-ankylosaurine ankylosaurids (Arbour and Currie 2016; Wiersma and Irmis 2018; Raven et al. 2023). Some taxa have swapped positions among all these three regions of the ankylosaur tree (Tab. 1: *Cedarpelta, Gargoyleosaurus, Hylaeosaurus, Kunbarrasaurus, Liaoningosaurus, Mymoorapelta*). Not only are their positions drastically different between analyses based on different datasets, they tend to shift from one stem to another based on the same dataset with a slight modification to taxon/character sampling. In our analyses, the addition of *Datai* was enough to make a difference from a previous analysis of the base dataset (Tab. 1). *Hylaeosaurus* and *Kunbarrasaurus* were resolved as non-ankylosaurine ankylosaurids in Zheng et al. (2018) but they sit among non-euankylosaur ankylosaurs in this study. *Jinyunpelta* is resolved as a non-ankylosaurine in this study even though the analysis of our base dataset by Raven et al. (2023) produced a consistent result with different versions of the dataset from Zheng et al. (2018) (Tab.1). It is also interesting that in all the latter three analyses Asian ankylosaurines were paraphyletic, whereas in this study they formed a clade (with a couple of North American taxa nested within) (Tab. 1). These observations are interpreted in the same context with the facts that: a) all internal branches in Figure 6 have a decay index = 1, despite a long list of apomorphies on each branch; and b) the low consistency and retention indices indicate high rates of homoplasies.

Nevertheless, the two lines of analyses broadly converged on resolving *Datai* within the Ankylosaurinae, either in the grade (Fig. 6A) or the clade (Fig. 6B) of Asian taxa. It is closely allied with *Pinacosaurus*, which sits either more proximal to *Ankylosaurus* than or sister to *Datai*. This consistency implies robust support for the phylogenetic position of *Datai*. The relationships are each supported by an extensive list of anatomical characters in *Datai* shared with *Pinacosaurus* or with other ankylosaurines in general (bold typeface for A2, 3 and B2, 3: Tab. 2). None of these characters is unique to respective clades among ankylosaurs. However, some of the apomorphies identified in the dataset of Raven et al. (2023) are informative to distinguish *Datai* and *Pinacosaurus* from other Asian ankylosaurines because these character states do not typically occur in derived ankylosaurines. These characters include the absence of median notch on the premaxilla (in the dataset from Raven et al. 2023: 16.0) and the presence of paranasal apertures (36.1).

Datai is set apart from other ankylosaurines by an extensive list of autapomorphies (Tab. 2). These character states occur elsewhere in the ankylosaur trees and are prone to homoplasy to various degrees. Interestingly, some of these characters may be interpreted anatomically primitive and ontogenetically or allometrically controlled. For the dataset derived from Raven et al. (2023), these characters are: a relatively long skull (6.0), slender humerus (204.0), relatively small jugal/quadratojugal horn (302.0). For the dataset derived from Zheng et al. (2018), these characters are: premaxillary palate subtriangular and longer than wide (10.0, 11.0) and coracoid not fused to scapula. *Datai yingliangis* is based on two specimens that are considered ontogenetically immature. We discuss our general coding strategies for ontogenetically variable characters in the following subsection. Here, it suffices to say that these character states optimized as autapomorphic to *Datai* are different from the states assigned to the close relative *Pinacosaurus grangeri*, which was mainly coded on juvenile and subadult specimens. Some of these specimens are arguably younger ontogenetically and smaller in size than YLSNHM 01002 and YLSNHM 01003 (Maryańska 1971; Hill et al. 2003; Burns et al. 2011, 2015; Currie et al. 2011). Therefore, it is reasonable to consider these autapomorphic states as morphological differences independent of ontogenetic influences.

Overall, the two lines of maximum parsimony analyses agree on a clade of derived ankylosaurines from the Campanian and Maastrichtian North America to have arisen from the primarily Asian radiation (Arbour and Currie 2016; Raven et al. 2023). They differ in whether derived ankylosaurines from Asia represent an independent lineage largely endemic to that continent (Fig. 6B) or successive divergence events (Fig. 6A). *Datai* may be placed in the continuum of Asian ankylosaurines toward more derived, chronologically later forms (Fig. 6A) or as a morphologically primitive sister lineage to *Pinacosaurus* (Fig. 6B). The Coniacian–Turonian age for the Zhoutian Formation seems more consistent with the former scenario. In that consensus tree (Fig. 6A), *Crichtonpelta* (Sunjiawan Formation, Cenomanian) and *Jinyunpelta* (Liangtoutang Formation, Albian–Cenomanian) are nested just out-

Table 1. Comparison of different phylogenetic hypotheses on ankylosaurian taxa that have been unstable. The top header row indicates the source of the original data matrix. The second header row shows distinct analyses

| Taxa | Arbour & Currie (2016) | | Raven et al. (2023) | |
	Zheng et al. (2018)	This study	Raven et al. (2023)	This study
'Nodosauridae'	A clade	A clade	A grade	A grade
Mymoorapelta	Nodosaurid; forming a clade with *Dongyuangopelta* near the nodosaurid base	–	'Nodosaurid' grade; forming a clade with *Borealopelta* and *Stegopelta*	'Nodosaurid' grade; forming a clade with *Peloroplites*, *Animantarx*, *Gargoyleosaurus*, and *Gastonia*
Kunbarrasaurus	Non-ankylosaurine ankylosaurid	Non-euankylosaur ankylosaur	Shamosaurine	Non-ankylosaurine ankylosaurid
Hylaeosaurus	Non-ankylosaurine ankylosaurid	Non-euankylosaur ankylosaur	'Nodosaurid' grade; forming a clade with *Gastonia*, *Peloroplites*	–
Gargoyleosaurus	Nodosaurid	Non-euankylosaur ankylosaur	Non-euaukylosaur ankylosaur	'Nodosaurid' grade'; forming a clade with *Gastonia*, *Mymoorapelta*, *Animantarx*, and *Peloroplites*
Animantarx - Peloroplites	Distantly related within nodosaurids	Distantly related within nodosaurids	Animantarx as non-euankylosaur ankylosaur	Successive branches within the 'nodosaurid' grade
Europelta	In polytomy with *Struthiosaurus, Stegopelta, Pawpawsaurus, Hungarosaurus*	In polytomy with the *Denversaurus-Edmontonia* complex	In polytomy with *Borealopelta, Hungarosaurus, Pawpawsaurus, Polacanthus, Struthiosaurus*	In polytomy with *Borealopelta, Hungarosaurus, Pawpawsaurus, Polacanthus, Struthiosaurus*
Denversaurus-Edmontonia-Panoplosaurus complex	*Panoplosaurus* in polytomy	Grade	A clade	A clade
Tatankacephalus	In polytomy with *Nodosaurus, Silvisaurus, Niobrarasaurus, Ahshislepelta*	Nodosaurid; constrained by *Struthiosaurus* and *Hungarosaurus*	In the 'nodosaurid' grade; forming a clade with *Sauropelta*	In the 'nodosaurid' grade; forming a clade with *Sauropelta*
Cedarpelta	Non-ankylosaurine ankylosaurid	Non-ankylosaurine ankylosaurid	Non-euankylosaur ankylosaur	Non-euankylosaur ankylosaur
Liaoningosaurus	Non-ankylosaurine ankylosaurid	Non-ankylosaurine ankylosaurid	Shamosaurine	Non-euankylosaur ankylosaur
Shamosaurines	Polytomy	A clade	A clade	A grade
Jinyunpelta	Ankylosaurine	Ankylosaurine	Ankylosaurine	Non-ankylosaurine ankylosaurid
Asian ankylosaurines	Paraphyletic	Paraphyletic	Paraphyletic	In a clade (with *Akainacephalus* and *Ziapelta*)

Table 1 continued.

| Taxa | Arbour & Currie (2016) | | Raven et al. (2023) | |
	Zheng et al. (2018)	This study	Raven et al. (2023)	This study
Crichtonpelta	Ankylosaurine constrained by *Jinyunpelta* and *Pinacosaurus*	Ankylosaurine; forming a clade with *Datai*	Ankylosaurine; forming a clade with *Akainacephalus* and *Ziapelta*	Ankylosaurine; forming a clade with *Ziapelta*
Talarurus	Ankylosaurine; forming a clade with *Nodocephalosaurus*	Ankylosaurine; forming a clade with *Nodocephalosaurus*	Non-ankylosaurine ankylosaurid	Ankylosaurine; forming a clade with *Tsagantegia* and *Zaraapelta*

Table 2. List of apomorphies for selected clades generated by the two lines of maximum parsimony analyses (see main text for specific methodology). Each node is labeled in Figure 6. In the list of apomorphies, the characters are listed under three different constraining criteria: unambiguous character changes, ACCTRAN (accelerated transformation; optimized for the earliest possible changes given ambiguity), and DELTRAN (delayed transformation; optimized for the latest possible changes given ambiguity). Bold typeface indicates the character states present in *Datai yingliangis*. Italic typeface indicates characters for which in *Datai* differs in states (shown in parentheses). Grey font indicates characters missing in *Datai*, therefore unavailable for comparison. Arabic numerals are character number followed by state (1.0 means character 1, state 0).

	Zheng et al. (2018) + *Datai*	Raven et al. (2023) + *Datai*
Ankylosauridae (Figure 6: **A1, B1**)	Unambiguous: **2.1: Laterotemporal fenestra, invisible laterally** 75.1: Basisphenoid with transverse ridge **89.1, 90.1: Maxillary and dentary tooth crown, rounded and with fewer than 13 denticles** **115.1: Cranioventral process of coracoid** 132.1: Short postacetabular ilium 135.1: Ischium convex dorsally ACCTRAN: **10.0: Premaxillary palate, longer than wide** **16.1: External naris, obscured in dorsal view** **54.1: Well-developed nuchal margin** **86.1: Mandibular caputegulum greater than three quarters of mandibular length** **109.1: Zygapophyseal length greater than half centrum in posterior vertebrae** 124.1: Fused sternal plates 143.1: Manual unguals, hoof-shaped, triangular in dorsal view **164.1: First cervical half ring, four to six primary osteoderms** 170.1: Lateral thoracic osteosderms, ovoid DELTRAN: **20.1: Rugose frontonasal/parietal ornamentation** 149.1: Fourth trochanter, distal on femur 150.1: Tibia, wider distally 152.2: Three pedal digits	Unambiguous: **7.0: Nuchal width greater than interorbital width** **33.1: Nasal embayment, anterolaterally** *45.1* (**45.2**): *Two palpebrals/supraorbitals* *58.1* (**58.2**): *Parietal, flat* *67.0* (**67.0**): *Quadrate, slightly inclined* 202.1: Deltopectoral crest, greater than half the humeral length 248.0: Greater trochanter continuous from femoral head **297.1, 298.1: Squamosal/postorbital horn, extending posterodorsally short of nuchal margin** 318.2: Cervical half rings composed on osteoderms and underlying bony band segments 325.0: Ossicles absent ACCTRAN: **2.1: Lateral temporal fenestra absent** **9.1: Skull roof, arched anteriposteriorly** **25.1: Tall maxilla** **52.1: Lacrimal, vertical** **96.0: Jaw joint, posterior to adductor fossa** *138.0* (**138.1**): *Postzygapophysis on posterior cervical vertebrae, short* 159.1: Ribs fused to posterior dorsal vertebrae 160.0: Longitudinal groove on the ventral side of sacral vertebra 184.1: Inverted 'T'-shaped haemal spines 198.0: Scapula, dorsal margin straight 199.1: Fused sternal plates

Table 2 continued.

	Zheng et al. (2018) + *Datai*	Raven et al. (2023) + *Datai*
		208.1: Humerus, bulged attachment for deltoid musculature
		263.1: Pedal digit IV, three or fewer phalanges
		273.1: Skull roof caputegulae, pyramidal
		302.1 (**302.0**): *Jugal/quadratojugal horn, base greater than orbital length*
		326.0: Pectoral osteoderms
		332.1: Triangular caudal osteoderms
		333.1: Tail club
		DELTRAN:
		16.1 (**16.0**): *Premaxilla, median notch*
		80.1: Paroccipital process, extending laterally
		112.1: Foramina on predentary
		122.6: Premaxilla, edentulous
		304.1: Jugal/quadratojugal horns longer than squamosal/postorbital horns
Ankylosaurinae (Figure 6: **A2, B2**)	Unambiguous:	Unambiguous:
	38.2: Supraorbitals forming a ridge	**58.2: Parietal, concave dorsal surface**
	40.1: Oblique long axis of orbit	**268.1: Cranial caputegulae**
	176.1, 177.1: Tail club longer than wide, with semicircular osteoderms	279.1: Supranarial caputegulae
		283.2: Loreal and lacrimal caputegulae
		303.0: Jugal/quadratojugal horn, not obscuring quadrate
	ACCTRAN:	
	10.1 (**10.0**): *Premaxillary palate wider than long*	ACCTRAN:
	13.1: Premaxillary tomium extending to maxilla	*14.1* (**14.2**): *Premaxillary palate longer than wide*
		281.1: A single internarial caputegulum
	DELTRAN:	330.0: Unfused pelvic osteoderms
	9.1: Premaxillary sinus	
	18.1: Looped nasal airway	DELTRAN:
	56.1: Inclined quadrate shaft	*19.0* (**19.1**): *Premaxilla, tall*
	68.1: Vomer contacting skull roof	37.1: Looped nasal airway
	101.1: Ribs fused to posterior dorsal vertebrae	**46.1: Supraorbitals forming a ridge**
	119.1: Pronounced glenoid lip on scapula	**72.0: Quadrate fossa**
	120.1: Acromion process forming a flange	81.1: Basal tubera as a continuous transverse ridge
	133.1: Pubis indistinct from ilium	**114.1, 119.1: Rounded and symmetrical tooth crown**
	167.1: Small inter-osteoderm ossicles in regions outside pelvis	160.0: Longitudinal groove on the ventral side of sacral vertebra
		180.1: Zygapophyseal length greater than half centrum in posterior caudal vertebrae
		199.1: Fused sternal plates
		208.1: Humerus, bulged attachment for deltoid musculature
		235.1: Pubis fused on ilium/ischium
		243.2: Ischium, convex proximal margin
		251.2: Fourth trochanter absent
		258.1: Tibia and astragalus, fused
		263.1: Pedal digit IV, three or fewer phalanges
		271.3: More than 30 caputegulae on skull roof
		273.1: Skull roof caputegulae, pyramidal

Table 2 continued.

	Zheng et al. (2018) + *Datai*	Raven et al. (2023) + *Datai*
		291.2: Two nuchal caputegulae **307.1: Mandibular caputegulum deeper than lower mandibular margin** 333.1: Tail club
The least inclusive clade containing both *Datai* and *Pinacosaurus* (Figure 6: **A3, B3**)	Unambiguous: **32.1: Posterior palatal foramen** **35.1: Lacrimal caputegulum** *53.1* (**53.2**): *Two nuchal caputegulae* **58.1: Ventral extreme of quadrate behind quadratojugal** **69.1: Pterygoid foramen** **108.1: Haemal arches fused to centra** ACCTRAN: 138.1: deltopectoral crest greater than half of humeral length 151.1: Astragalus and tibia forming a suture DELTRAN: **13.1: Premaxillary tomium extending onto maxilla** **86.1: Mandibular caputegulum longer than half the mandibular length** **114.1: Coracoid with gently convex anterior margin**	Unambiguous: **45.2: Three supraorbitals** **85.1: Pterygoid shield** **135.0: Anterior cervical centra, straight ventral margin** ACCTRAN: **14.2: Premaxillary palate wider than long** **67.2: Posteriorly inclined quadrate** 78.1: Occipital condyle, round 82.0: Basipterygoid process twice as long as wide 95.1: Posterior palatal foramen **105.0: Coronoid eminence low** **132.0: Cervical centra, anterior and posterior faces aligned** **140.0: Cervical ribs, unfused to centra** 162.2: Posterior sacral ribs, anterolateral 168.1: Anterior caudal centra, equidimensional **187.0: Coracoid, convex anterior margin** **213.0: Radius, slender** 246.0: Ischium, distal end expanded 270.0: Flat caputegulae on skull roof 274.1: Caputegulae on anterior skull roof closely demarcated 280.1: Supranarial caputegulae with a notch 281.2: Multiple internarial caputegulae 283.3: More than two caputegulae in loreal and lacrimal region **306.1: Mandibular caputegulum greater than half the mandibular length** 315.0: Flat base of osteoderms 322.0: Median osteoderm of cervical half ring, flat DELTRAN: **1.1: Antorbital fenestra absent** **16.0: Premaxilla, median notch absent** **36.1: Paranasal apertures**
Datai (autapomorphies)	Unambiguous: **7.1: Deep furrow in premaxilla** **11.0: Premaxillary palate subtriangular** **51.0: Flat parietal** **70.1: Pterygoid body medial to quadrate condyle** **168.0: Deeply excavated, flat triangular osteoderms absent** ACCTRAN: **6.0: flat antorbital region**	Unambiguous: **6.0: Skull longer than wide** **10.1: Skull tallest at orbit** **19.1: Premaxilla, low** **59.0, 60.0: Jugal, anterior process deep** **70.0: Pterygoid process deeper than half the height of quadrate** **92.0: Pterygovomerine keel above tooth row** **98.0: Dentary, symphysis deeper than main body** **109.0: Surangular, anterior lateral ridge absent**

Table 2 continued.

	Zheng et al. (2018) + *Datai*	Raven et al. (2023) + *Datai*
	10.0: Premaxillary palate longer than wide **28.0: Maxillary tooth row gently convex medially** **117.0: Coracoid not fused to scapula** DELTRAN: **167.1: Small ossicles**	**143.0: Longitudinal keel on the ventral side of dorsal vertebra** **150.0: Dorsal vertebrae, transverse process horizontal** **194.1: Scapulocoracoid, lateral buttress** **204.0: Humerus, distal width narrow** **302.0: Jugal/quadratojugal, base smaller than orbital length** ACCTRAN: **54.2: Frontal as long as wide** **134.0: Anterior cervical neural spines, tall** **138.1: Well-developed postzygapophyses on posterior cervical vertebra** **217.0: Metacarpal I, short** DELTRAN: **52.1: Lacrimal, vertical** **54.2: Frontal as long as wide** **63.0: Quadratojugal, dorsal process** **67.2: Quadrate, posteriorly inclined** **105.0: Coronoid eminence low** **306.1: Mandibular caputegulum greater than half the mandibular length**
The most inclusive clade of ankylosaurines that does not contain *Datai* (Figure 6: **A4, B4**)	Unambiguous: *4.1* (**4.0**): *Skull wider than long* *15.1* (**15.0**): *External naris opening anteriorly* *24.1* (**24.0**): *Notch in supranarial caputegulum* *30.1* (**30.0**): *Maxillary tooth rows narrowly separated from each other* *36.1* (**36.0**): *Flat prefrontal caputegulum* *156.2* (**156.1**): *Deeply excavated base of osteoderm* *161.0* (**161.1**): *Gular osteoderms absent* ACCTRAN: *27.1* (**27.0**): *A single loreal caputegulum* DELTRAN: *6.1* (**6.0**): *Arched antorbital region* *10.1* (**10.0**): *Premaxillary palate wider than long* *28.1* (**28.0**): *Maxillary tooth row medially convex* 92.1: Atlantal neural arch fused to intercentrum *117.1* (**117.0**): *Coracoid and scapula fused to each other* 124.1: Fused sternal plates 130.1: Laterally obscured acetabulum 138.1: Deltopectoral crest longer than half the humeral length 151.1: Astragalus and tibia forming a suture	Unambiguous: *67.3* (**67.2**): *Quadrate, strongly inclined posteriorly* *116.1* (**116.0**): *Teeth with central apical ridge* 173.0: Anterior caudal vertebrae, trasverse process anteriolateral 200.1: Deltopectoral crest separated from humeral head by a notch ACCTRAN: *26.2* (**26.0**): *Maxillary tooth rows, expanded posteriorly* *34.0* (**34.1**): *External naris, visible in dorsal view* 71.0: Quadrate fused with paroccipital process 95.1: Posterior palatal foramen **105.0: Coronoid eminence low** *147.1* (**147.0**): *Dorsal vertebrae, centra low* 164.3: Three caudosacral vertebrae 181.1, *182.1* (**182.0**), *183.0* (**183.1**): *Posterior caudal vertebrae*, equidimensional centra, *tongue-shaped postzygapophyses, transverse processes* *191.0* (**191.1**): *Scapula, glenoid ventrolateral* **194.1: Scapulocoracoid, lateral buttress** 201.1: Humerus, medial tubercle separated from humeral head by a notch 265.2: Pedal digit I, phalanges absent *285.1* (**285.0**): *Ciliary osteoderms* DELTRAN: 326.0: pectoral osteoderms absent

Table 2 continued.

	Zheng et al. (2018) + *Datai*	Raven et al. (2023) + *Datai*
The 'Asian' ankylosaurine clade (Figure 6: **A5, B5**)	Unambiguous: *63.1* (**63.0**): *Paroccipital process fused to quadrate* ACCTRAN: *82.1* (**82.0**): *Distinct coronoid process* 94.1: Fused atlas and axis 136.1: Humeral head and deltopectoral crest separated by a distinct notch DELTRAN: *21.2* (**21.0**): *Eleven to 30 caputegulae in prefrontal and frontonasal region*	Unambiguous: 77.0: Occipital condyle, posterior 83.1: Basiocipital-basisphenoid, medial depression 84.1: Three foramina for cranial nerve XII **121.0: Fewer than 20 teeth per row** **186.0: Coracoid as tall as long** 222:1: Ilium, anterior iliac process with ventral curvature **300.1: Jugal/quadratojugal horn, triangular** ACCTRAN: **16.0: Premaxilla, median notch absent** **36.1: Paranasal apertures** 38.0: Vascular impressions on nasal cavity *132.2* (**132.0**): *Cervical vertebrae, anterior and posterior faces offset dorsoventrally* 161.2: Four sacral vertebrae *187.1* (**187.0**): *Coracoid, straight anterior margin* 209.0: Ulna, short 254.1: Femur, long 270.2: Bulbous caputegulae on skull roof DELTRAN: **130.0: Seven cervical vertebrae** **147.0: Dorsal centra low** 159.1: Ribs fused to posterior dorsal vertebrae 281.1: Single internarial caputegulum

side *Datai* and the rest of ankylosaurines. However, the Cenomanian age for the Baynshire Formation in which *Talarurus* and *Tsagantegia* occur implies the origin of derived ankylosaurines deeper into the mid-Cretaceous times. Therefore, the latter scenario (*Datai* as a morphologically primitive derived ankylosaurine) is not to be ruled out. Regardless of whichever interpretations are correct, the discovery of *Datai* suggests that the early Late Cretaceous of Asia harboured a diverse array of ankylosaurids that document the transitions across the origin of the Ankylosaurinae. Improved sampling and better anatomical/systematic understanding in this region will be critical to understand early evolution of these iconic Late Cretaceous armoured dinosaurs with a tail club.

Ontogenetic Status of YLSNHM 01002 and Character Scoring: The relatively primitive morphology and early branching of *Datai yingliangis* with respect to other post-Cenomanian ankylosaurines might be an artifact of the immature status of the type specimens. However, the coding for *Datai* is consistent with how other ankylosaurs were coded based on immature specimens, and some seemingly juvenile features in *Datai* appear to be genuine plesiomorphies. The characters related to overall skull profile (in the dataset from Zheng et al., 2018: width to length, 4.0; antorbital region, 6.0; premaxillary palate, 10.0, 11.0; maxillary tooth row, 28.0) are variably coded in other ankylosaurs known from juvenile specimens (*Chuanqilong chaoyangenis, Liaoningosaurus paradoxus, Pinacosaurus grangeri*). These states in *Datai* occur in the grade that includes shamosaurines and *Jinyunpelta*, except for Character 11 (premaxillary palate, shape). In addition to these, *Datai* lacks dermal ossification that would be present a fully adult post-Cenomanian ankylosaurine (in the dataset from Zheng et al., 2018: 21.0, 22.0, 24.0, 26.0, 27.0, 36.0, 48.1, 86.1, 164.1) and fusion in scapulocoracoid (117.0). Rather than treated ambiguously (with missing [?] or inapplicable [-]), these characters were coded for the morphology present in the specimens in accordance with the other ankylosaurids known from immature specimens (*C. chaoyangensis, L. paradoxus, P. grangeri*). It would be a valuable experiment to test different coding strategies on potentially ontogenetically influenced characters, but such a comprehensive re-analysis is beyond the scope of this paper.

Here, we discuss two plesiomorphic states in the dermal ossification of *Datai yingliangis* with respect to derived ankylosaurines: the absence of loreal caputegulum (27.0 in the dataset from Zheng et al., 2018) and the small size of the jugal/quadratojugal horns (48.1). Comparison with juveniles of *Pinacosaurus grangeri* suggests that these characters are each an ontogenetically terminal state as expressed in YLSNHM 01002. In juvenile specimens of *P. grangeri* (IGM 100/1014, ZPAL MgD-II/1), dermal ossification is present in the position corresponding to a loreal caputegulum, but the lacrimal caputegulum appears to be in its earliest stage of development (Maryańska 1971; Hill et al. 2003). In YLSNHM 01002, the lacrimal caputegulum is clearly differentiated, but there is no indication of dermal ossification in the loreal position. Similarly, the jugal/quadratojugal horns are prominent already in those juvenile specimens of *P. grangeri*, but in YLSNHM 01002 the horns are small and dual. The plesiomorphies regarding the osteoderm composition (163.0 in the dataset from Zheng et al., 2018) and the osteodermal base (168.0, 169.0) in *D. yingliangis* may be attributed to the fact that so few trunk osteoderms are preserved in YLSNHM 01002 and YLSNHM 01003. Perhaps these elements are absent, missing, or yet to develop in these specimens. At any rate, the morphological differences from *Crichtonpelta* and *Jinyunpelta* as described in Results are considered independent of ontogenetic transformations.

Implications for Behavior:

The two specimens of *Datai yingliangis* were found in association, with the head of YLSNHM 01003 resting on top of that of YLSNHM 01002. Similarly, articulated juvenile specimens of *Pinacosaurus grangeri* from the Djadokhta localities (Alag Teeg, Bayan Mandahu, Ukhaa Tolgod) have been found together in an apparent rapid burial event with no evidence of postmortem transport (Jerzykiewicz et al. 1993; Hill et al. 2003; Burns et al. 2011, 2015; Currie et al. 2011). Based on the sandy or muddy facies and the upright posture, those from Bayan Mandahu have been interpreted as potentially buried in a sandstorm (Jerzykiewicz et al. 1993), and those from Alag Teeg posited as mired in mud (Currie et al. 2011). Limited information is available for YLSNHM 01002 and YLSNHM 01003. Much of their postcranial skeletons was likely destroyed during the construction process, and it remains unclear whether other individuals were preserved at the site. The preservation of these two specimens in a burrow (Park et al. 2021) was considered as another possibility, but there is no evidence for such a structure in the block from which the specimens were extracted. The Zhoutian succession is generally interpreted as having been deposited in fluvial to lacustrine settings with no apparent aeolian features (Yu and Fan 2022). The data available at hand are consistent with the hypothesis that juvenile ankylosaurids are gregarious (Currie et al. 2011).

ACKNOWLEDGEMENTS

Author Contributions: L.X. and K.N. conceived and designed this study; K.N. acquired the type materials of *Datai yingliangis*; L.X. conducted geological survey of the type locality; T.M. and L.X. collected data and conducted anatomical comparison; T.M. executed phylogenetic analysis, prepared figures, and wrote the manuscript with input from J.C.M. and L.X. All authors participated in discussion of the ideas presented in this paper and approved final version of the manuscript.

Supplementary Information

Supplementary data 1. Dataset from Zheng et al. (2018) with the addition of *Datai yingliangis*.

Supplementary data 2. Dataset from Raven et al. (2023) with the addition of *Datai yingliangis*.

Supplementary data 3. PAUP output for the list of apomorphies based on the dataset from Zheng et al. (2018).

Supplementary data 4. PAUP output for the list of apomorphies based on the dataset from Raven et al. (2023).

These supplementary data files are available at DOI: 10.6084/m9.figshare.25036052 as well as the journal website.

LITERATURE CITED

Arbour, V.M., and P.J. Currie. 2013. *Euoplocephalus tutus* and the diversity of ankylosaurid dinosaurs in the Late Cretaceous of Alberta, Canada, and Montana, USA. Plos One 8:e62421. DOI 10.1371/journal.pone.0062421.

Arbour, V.M., and P.J. Currie. 2015. Ankylosaurid dinosaur tail clubs evolved through stepwise acquisition of key features. Journal of Anatomy 227:514–523. DOI 10.1111/joa.12363.

Arbour, V.M., and P.J. Currie. 2016. Systematics, phylogeny and palaeobiogeography of the ankylosaurid dinosaurs. Journal of Systematic Palaeontology 14:385–444. DOI 10.1080/14772019.2015.1059985.

Arbour, V.M., and D.C. Evans. 2017. A new ankylosaurine dinosaur from the Judith River Formation of Montana, USA, based on an exceptional skeleton with soft tissue preservation. Royal Society Open Science 4:161086. DOI 10.1098/rsos.161086.

Backwell, L.R., A.H. Parkinson, E.M. Roberts, F. d'Errico, and J.-B. Huchet. 2012. Criteria for identifying bone modification by termites in the fossil record. Palaeogeography, Palaeoclimatology, Palaeoecology 337–338:72–87. DOI 10.1016/j.palaeo.2012.03.032.

Britt, B.B., R.D. Scheetz, and A. Dangerfield. 2008. A suite of dermestid beetle traces on dinosaur bone from the Upper Jurassic Morrison Formation, Wyoming, USA. Ichnos 15:59–71. DOI 10.1080/10420940701193284.

Bureau of Geology and Mineral Resources of Jiangxi Province. 1984. Regional Geology of Jiangxi Province. Geological Publishing House, Beijing.

Burns, M.E., P.J. Currie, R.L. Sissons, and V.M. Arbour. 2011. Juvenile specimens of Pinacosaurus grangeri Gilmore, 1933 (Ornithischia: Ankylosauria) from the Late Cretaceous of China, with comments on the specific taxonomy of Pinacosaurus. Cretaceous Research 32:174–186. DOI 10.1016/j.cretres.2010.11.007.

Burns, M.E., T.A. Tumanova, and P.J. Currie. 2015. Postcrania of juvenile Pinacosaurus grangeri (Ornithischia: Ankylosauria) from the Upper Cretaceous Alagteeg Formation, Alag Teeg, Mongolia: implications for ontogenetic allometry in ankylosaurs. Journal of Palaeontology 89:168–182. DOI 10.1017/jpa.2014.14.

Carpenter, K. 2001. Phylogenetic analysis of the Ankylosauria; pp. 455-483 in K. Carpenter (ed.), Armored Dinosaurs. Indiana University Press, Bloomington.

Coombs, W. 1995. A new nodosaurid ankylosaur (Dinosauria, Ornithischia) from the Lower Cretaceous of Texas. Journal of Vertebrate Paleontology 15:298–312. DOI 10.1080/02724634.1995.10011231.

Coombs, W.P. 1978. The families of the ornithischian dinosaur order Ankylosauria. Palaeontology 21:143–170.

Coombs, W.P. 1986. A juvenile ankylosaur referable to the genus Euoplocephalus (Reptilia, Ornithischia). Journal of Vertebrate Paleontology 6:162–173.

Currie, P.J., D. Badamgarav, E.B. Koppelhus, R. Sissons, and M.K. Vickaryous. 2011. Hands, feet, and behaviour in Pinacosaurus (Dinosauria: Ankylosauridae). Acta Palaeontologia Pololonica 56:489–504. DOI 10.4202/app.2010.0055.

Godefroit, P., X. Pereda Suberbiola, H. Li, and Z.-M. Dong. 1999. A new species of the ankylosaurid dinosaur Pinacosaurus from the Late Cretaceous of Inner Mongolia (P.R. China). Bulletin de l'Institut Royal des Sciences Naturelles de Belqique, Sciences de la Terre 69:17–36.

Han, F., W. Zheng, D. Hu, X. Xu, and P.M. Barrett. 2014. A new basal ankylosaurid (Dinosauria: Ornithischia) from the Lower Cretaceous Jiufotang Formation of Liaoning Province, China. PLoS ONE 9:e104551. DOI 10.1371/journal.pone.0104551.

Hill, R.V., L.M. Witmer., and M.A. Norell. 2003. A new specimen of Pinacosaurus grangeri (Dinosauria: Ornithischia) from the Late Cretaceous of Mongolia: Ontogeny and phylogeny of ankylosaurs. American Museum Novitates 3395:1–29. DOI 10.1206/0003-0082(2003)395<0001:ANSOPG>2.0.CO;2.

Jerzykiewicz, T., P.J. Currie, D.A. Eberth, P.A. Johnston, E.H. Koster, and J.-J. Zheng. 1993. Djadokhta Formation correlative strata in Chinese Inner Mongolia: An overview of the stratigraphy, sedimentary geology, and paleontology and comparisons with the type locality in the pre-Altai Gobi. Canadian Journal of Earth Sciences 30:2180–2195. DOI 10.1139/e93-190.

Jiangxi Bureau of Geology and Mineral Resources. 1987. Regional Geology of Jiangxi province. The Ministry of Geology and Mineral Resources, Beijing.

Jiangxi Bureau of Geology and Mineral Resources. 1997. Lithostratigraphy of Jiangxi province. China University of Geosciences Press, Wuhan.

Jiangxi Geological Survey and Mineral Survey Brigade. 1991. Report of regional geological survey of Huichang Sheet at the scale of 1: 50000. Nanchang Bureau of Geology and Mineral Resources, Nanchang.

Kirkland, J.I. 1998. A polacanthine ankylosaur (Ornithischia: Dinosauria) from the Early Cretaceous (Barremian) of eastern Utah. New Mexico Museum of Natural History Bulletin 14:271–281.

Kirkland, J.I., K. and Bader. 2010. Insect trace fossils associated with Protoceratops carcasses in the Djadokhta Formation (Upper Cretaceous), Mongolia; pp. 509–519 in M.J. Ryan, B.J. Chinnery-Allgeier, and D.A. Eberth (eds.), New Perspectives on Horned Dinosaurs. Indiana University Press, Bloomington.

Kuzmin, I., I. Petrov., A. Averianov, E. Boitsova, P. Skutschas, and H.-D. Sues. 2020. The braincase of Bissektipelta archibaldi — new insights into endocranial osteology, vasculature, and paleoneurobiology of ankylosaurian dinosaurs. Biology Communications 65:85–156. DOI 10.21638/spbu03.2020.201.

Li, F., S. Bi, M. Pittman., S.L. Brusatte, and X. Xu. 2016. A new tyrannosaurine specimen (Theropoda: Tyrannosauroidea) with insect borings from the Upper Cretaceous Honglishan Formation of Northwestern China. Cretaceous Research 66:155–162. DOI 10.1016/j.cretres.2016.06.002.

Li, J., Zhang, Y., S. Dong, and S.T. Johnston. 2014. Cretaceous tectonic evolution of South China: A preliminary synthesis. Earth-Science Reviews 134:98–136. DOI 10.1016/j.earscirev.2014.03.008.

Li, X.-H, C.-K. Zhang, Y. Wang, and L. Liu. 2018. Geochronostratigraphy and Relationship of the Late Mesozoic terrestrial lithostatigraphic units in South China. Acta Geologica Sinica 92:1107–1130.

Ling, L.-H. 1996. Establishment of the Cretaceous Formations of Maodian, Hekou and Tangbian in Jiangxi Province. Geological Science and Technology of Jiangxi 23:55–59.

Lü, J., Ji, Q., Y. Gao, and Z. Li. 2007a. A new species of the ankylosaurid dinosaur *Crichtonsaurus* (Ankylosauridae: Ankylosauria) from the Cretaceous of Liaoning Province, China. Acta Geologica Sinica 81:883–897.

Lü, J., X. Jin, Y. Sheng, Y. Li, G. Wang, and Y. Azuma. 2007b. New nodosaurid dinosaur from the Late Cretaceous of Lishui, Zhejiang Province, China. Acta Geologica Sinica – English Edition 81:344–350. DOI 10.1111/j.1755-6724.2007. tb00958.x.

Maryańska, T. 1971. New data on the skull of *Pinacosaurus grangeri*. Palaeontologia Polonica 25:45–53.

Maryańska, T. 1977. Ankylosauridae (Dinosauria) from Mongolia. Palaeontologia Polonica 37:85–151.

Norman, D.B. 2021. *Scelidosaurus harrisonii* (Dinosauria: Ornithischia) from the Early Jurassic of Dorset, England: Biology and phylogenetic relationships. Zoological Journal of the Linnean Society 191:1–86. DOI 10.1093/zoolinnean/zlaa061.

Osi, A. 2005. *Hungarosaurus tormai*, a new ankylosaur (Dinosauria) from the Upper Cretaceous of Hungary. Journal of Vertebrate Paleontolology 25:370–383. DOI 10.1671/0272-4634(2005)025[0370:HTANAD]2.0.CO;2.

Park, J.-Y., Y.-N. Lee, P.J. Currie, Y. Kobayashi, E. Koppelhus, R. Barsbold, O. Mateus, S. Lee, and S.-H. Kim. 2020. Additional skulls of *Talarurus plicatospineus* (Dinosauria: Ankylosauridae) and implications for paleobiogeography and paleoecology of armored dinosaurs. Cretaceous Research 108:104340. DOI 10.1016/j.cretres.2019.104340.

Park, J.-Y., Y.-N. Lee, P.J. Currie, M.J. Ryan, P. Bell, R. Sissons, E.B. Koppelhus, R. Barsbold, S. Lee, and S.-H. Kim. 2021. A new ankylosaurid skeleton from the Upper Cretaceous Baruungoyot Formation of Mongolia: its implications for ankylosaurid postcranial evolution. Scientific Reports 11:4101. DOI 10.1038/s41598-021-83568-4.

Raven, T.J., P.M. Barrett, C.B. Joyce, and S.C.R. Maidment. 2023. The phylogenetic relationships and evolutionary history of the armoured dinosaurs (Ornithischia: Thyreophora). Journal of Systematic Palaeontology 21:2205433. DOI 10.1080/14772019.2023.2205433.

Riguetti, F., X. Pereda-Suberbiola, D. Ponce, L. Salgado, S. Apesteguía, S. Rozadilla, and V. Arbour. 2022a. A new small-bodied ankylosaurian dinosaur from the Upper Cretaceous of North Patagonia (Río Negro Province, Argentina). Journal of Systematic Palaeontology 20:2137441. DOI 10.1080/14772019.2022.2137441.

Riguetti, F.J., S. Apesteguía, and X. Pereda-Suberbiola. 2022b. A new Cretaceous thyreophoran from Patagonia supports a South American lineage of armoured dinosaurs. Scientific Reports 12:11621. DOI 10.1038/s41598-022-15535-6.

Rivera-Sylva, H.E., E. Frey, W. Stinnesbeck, G. Carbot-Chanona, I.E. Sanchez-Uribe, and J.R. Guzmán-Gutiérrez. 2018. Paleodiversity of Late Cretaceous Ankylosauria from

Mexico and their phylogenetic significance. Swiss Journal of Palaeontology 137:83–93. DOI 10.1007/s13358-018-0153-1.

Sereno, P.C. 1998. A rationale for phylogenetic definitions, with application to the higher level taxonomy of Dinosauria. Neues Jahrbuch für Geologie und Paläontologie Abhandlungen 210:41–83.

Serrano-Brañas, C.I., B. Espinosa-Chávez, and S.A. Maccracken. 2018. Insect damage in dinosaur bones from the Cerro del Pueblo Formation (Late Cretaceous, Campanian) Coahuila, Mexico. Journal of South American Earth Sciences 86:353–365. DOI 10.1016/j.jsames.2018.07.002.

Soto-Acuña, S., A.O. Vargas, J. Kaluza, M.A. Leppe, J.F. Botelho, J. Palma-Liberona, C. Simon-Gutstein, R.A. Fernández, H. Ortiz, V. Milla, B. Aravena, L.M.E. Manríquez, J. Alarcón-Muñoz, J.P. Pino, C. Trevisan, H. Mansilla, L.F. Hinojosa, V. Muñoz-Walther, and D. Rubilar-Rogers. 2021. Bizarre tail weaponry in a transitional ankylosaur from subantarctic Chile. Nature 600(7888):259–263. DOI 10.1038/s41586-021-04147-1.

Swofford, D.L. 2002. PAUP: phylogenetic analysis using parsimony (and other methods). Version 4.0a (build 167, February 1 2020). Sinauer Associates, Inc., Sunderland, Massachusetts.

Thompson, R.S., J.C. Parish, S.C.R. Maidment, and P.M. Barrett. 2012. Phylogeny of the ankylosaurian dinosaurs (Ornithischia: Thyreophora). Journal of Systematic Palaeontology 10:301–312. DOI 10.1080/14772019.2011.569091.

Tumanova, T.A. 1987. [The armored dinosaurs of Mongolia]. Trudy Sovmestnoi Sovestsko-Mongol'skoi Paleontologischeskoi Expeditsii 32:1–76. [in Russian]

Vickaryous, M.K., T. Maryańska, and D.B. Weishampel. 2004. Ankylosauria; pp. 157–186 in D.B. Weishampel, P. Dodson, and H. Osmolska (eds.), The Dinosauria (2nd edition). University of California Press, Berkeley.

Vickaryous, M.K., A.P. Russell, P.J. Currie, and X.J. Zhao. 2001. A new ankylosaurid (Dinosauria: Ankylosauria) from the Lower Cretaceous of China, with comments on ankylosaurian relationships. Canadian Journal of Earth Sciences 38:1767–1780. DOI 10.1139/e01-051.

Wiens, J.J. 2003a. Incomplete taxa, incomplete characters, and phylogenetic accuracy: Is there a missing data problem? Journal of Vertebrate Paleontology 23:297–310. DOI 10.1671/0272-4634(2003)023[0297:ITICAP]2.0.CO;2.

Wiens, J.J. 2003b. Missing data, incomplete taxa, and phylogenetic accuracy. Systematic Biology 52:528–538. DOI 10.1080/10635150390218330.

Wiens, J.J. 2005. Can incomplete taxa rescue phylogenetic analyses from long-branch attraction? Systematic Biology 54:731–742. DOI 10.1080/10635150500234583.

Wiens, J.J., and J. Tiu. 2012. Highly incomplete taxa can rescue phylogenetic analyses from the negative impacts of limited taxon sampling. PLoS ONE 7:e42925. DOI 10.1371/journal.pone.0042925.

Wiersma, J.P., and R.B. Irmis. 2018. A new southern Laramidian ankylosaurid, *Akainacephalus johnsoni* gen. et sp. nov., from the

upper Campanian Kaiparowits Formation of southern Utah, USA. PeerJ 6:e5016. DOI 10.7717/peerj.5016.

Wu, W.-B., L.-Q. Chen, T. Ding, W.-H. Li, and Y.-J. Wang. 2020. Sedimentary characteristics and paleoclimate significance of the Late Cretaceous Zhoutian Formation Red Beds in the Guangfeng Basin. Acta Sedimentologica Sinica 38:485–496.

Xing, L., E.M. Roberts, J.D. Harris, M.K. Gingras, H. Ran, J. Zhang, X. Xu, M.E. Burns, and Z. Dong. 2013. Novel insect traces on a dinosaur skeleton from the Lower Jurassic Lufeng Formation of China. Palaeogeography, Palaeoclimatology, Palaeoecology 388:58–68. DOI 10.1016/j.palaeo.2013.07.028.

Yang, J., H. You., L. Xie, and H. Zhou. 2017. A new specimen of *Crichtonpelta benxiensis* (Dinosauria: Ankylosaurinae) from the Mid-Cretaceous of Liaoning Province, China. Acta Geologica Sinica, English edition 91:781–790. DOI 10.1111/1755-6724.13308.

Yao, X., P.M. Barrett, L. Yang, X. Xu, and S. Bi. 2022. A new early branching armored dinosaur from the Lower Jurassic of southwestern China. eLife 11:e75248. DOI 10.7554/eLife.75248.

Yu, C., and X. Fan. 2022. Distribution of dinosaur egg fossils and occurrence stratigraphic characteristics of Meilin—Maodian, Ganzhou Basin. Journal of Shijiazhuang University of Economics 45(4):6–12.

Yu C., X. Fan, and L. Zhong. 2020. Distribution of dinosaur egg fossils and occurrence stratigraphic characteristics of Yudu Basin, Southern Jiangxi. East China Geology 45:396–402. DOI 10.16788/j.hddz.32-1865/P.2020.04.011.

Zheng, W., X. Jin, Y. Azuma, Q. Wang, K. Miyata, and X. Xu. 2018. The most basal ankylosaurine dinosaur from the Albian–Cenomanian of China, with implications for the evolution of the tail club. Scientific Reports 8:3711. DOI 10.1038/s41598-018-21924-7.

Zou, S.-L., Q. Wang, and X.-L. Wang. 2013. A new oospecies of parafaveoloolithids from the Pingxiang Basin, Jiangxi Province of China. Vertebrata Palasiatica 51(2):102.

Appendix 1. Measurements from the type specimens of *Datai yingliangis* (YLSNHM 01002, YLSNHM 01003). Data units are in millimeters (mm).

	YLSNHM 01002	YLSNHM 01003
Skull length (snout-nuchal margin)	235	201
Skull width (across squamosals)	179	157
Skull width (across postorbitals)	168	152
Skull width (between orbits)	178	142
Orbit length (left, right)	47, 50	50, 49
Maxilla length (maximum)	115	109
Frontal length (along midline)	57	41
Frontal width (maximum)	89	70
Jugal length (maximum, horizontally)	83	69
Pterygoid width (left or right, maximum)	56	–
Dentary length (along ventral margin	139	108
Lower jaw length	225	193
Second cervical half ring, width (right side)	165	–
Coracoid width	116	91
Humerus, proximal width	–	81
Humerus, shaft width	48	–
Humerus, shaft circumference	117	–
Humerus, distal width	104	82
Ulna, proximal length	–	69
Ulna, proximal width	–	71
Ulna, distal width	–	46